EPJ Web of Conferences **146**, 05002 (2017) DOI: 10.1051/epjconf/201714605002
ND2016

A unified understanding of (γ,n) and (n,γ) reactions and direct neutron-multiplicity sorting

Hiroaki Utsunomiya[1,a], Stephane Goriely[2], Therese Renstrøm[3], Seitaro Katayama[1], Ioana Gheorghe[4,5], Dan Filipescu[4], Sergey Belyshev[6], Vladimir Varlamov[7], and the PHOENIX Collaboration for the IAEA-CRP F41032

[1] Department of Physics, Konan University, Okamoto 8-9-1, Kobe 659-8501, Japan
[2] Institut d'Astronomie et d'Astrophysique, Université Libre de Bruxelles, Campus de la Plaine, CP-226, 1050 Brussels, Belgium
[3] University of Oslo, Department of Physics, 0316 Oslo, Norway
[4] ELI-NP, "Horia Hulubei" National Institute for Physics and Nuclear Engineering (IFIN-HH), 30 Reactorului, 077125 Bucharest-Magurele, Romania
[5] University of Bucharest, Post Office Box MG-11, 077125 Bucharest-Magurele, Romania
[6] Lomonosov Moscow State University, Department of Physics, Moscow 119991, Russia
[7] Lomonosov Moscow State University, Skobeltsyn Institute of Nuclear Physics, Moscow 119991, Russia

Abstract. We discuss the γ-ray strength function toward a unified understanding of (γ,n) and (n,γ) reactions and propose a novel technique of direct neutron-multiplicity sorting to resolve the long-standing discrepancy between the Livermore and Scalya data of partial photoneutron cross sections.

1. Introduction

The γ-ray strength function (γSF) is a nuclear statistical quantity that governs electromagnetic processes in radiative neutron capture and photoneutron emission. In the statistical model, the (γ,n) and (n,γ) reaction cross sections are interconnected through the γSF and the Brink hypothesis linking the downward γSF in photo- deexcitation to the upward γSF in photoabsorption in the approximate equality [1]. An indirect method called the γ-ray strength function method [2] was devised for constraining radiative neutron capture cross sections for unstable nuclei of direct relevance to nuclear astrophysics and nuclear engineering. This method requires a systematic measurement of (γ,n) cross sections over an isotopic chain and uses known (n,γ) cross sections for qualification of the model γSF. Thus, this method leads to a unified understanding of (γ,n) and (n,γ) reaction cross sections over an isotopic chain. The method was applied to such isotopic chains as Zr [3], Sn [4], Mo [5] and more recently, Sm [6] and Nd [7].

The γSF can also be constructed by putting experimental data of (γ,n), (γ,γ') and particle-gamma coincidences together.

The IAEA-CRP F41032 was launched in 2016 as a 4-year project to generate a reference database for photon strength functions and update the photonuclear library, IAEA-TECDOC-1178 published in 2000 [8], the compilation and evaluation of photonuclear data for 164 isotopes of 48 elements from ^{2}H to ^{241}Pu. In this project, the main purpose of the update is to resolve the discrepancy between the Livermore and Saclay data of partial photoneutron cross sections compiled in the library by providing new reliable data.

The emergence of quasi-monochromatic γ-ray beams produced by Compton backscattering of laser photons from relativisitiv electrons has made these research activities feasible at the turn of the 21st century.

2. Laser compton scattering γ-ray beam

The laser-Compton scattering (LCS) from relativistic electrons converts a laser beam to a quasi- monochromatic γ-ray beam with an energy- amplification factor, $\sim 4\gamma^2$, where γ is the Lorentz factor, $\gamma = \mathrm{E}_e/\mathrm{mc}^2$. The Lorentz factor is about 2000 at the electron energy $\mathrm{E}_e = 1\,\mathrm{GeV}$. Thus, the amplification factor is $\sim$ 16 million, producing a $\sim$ 16 MeV γ-ray beam from a 1 eV ($\lambda = 1064\,\mathrm{nm}$) photon beam of a Nd:$YVO_4$ laser. The LCS γ-ray beam, whose energy varies with the square of the electron energy, is energy-tunable from 4 to 38 MeV (8 to 76 MeV) with the use of the $\lambda = 1064\,\mathrm{nm}$ (532 nm) photons at the NewSUBARU synchrotron radiation facility where the electron beam energy can be changed from 0.5 to 1.5 GeV. The LCS γ-ray beam is quasi-monochromatic with energy spreads essentially determined by the electron beam emittance and size of the collimator. A typical energy spread is 1–2% in FWHM in photoneutron cross section measurements around neutron threshold [6,7]. The LCS γ-ray beam is background-free in the quasi-monochromatic region, which is in sharp contrast to the fact that γ-ray beams produced by the positron annihilation in flight are accompanied by considerable background γ-rays generated by the positron bremsstrahlung [9].

[a] e-mail: hiro@konan-u.ac.jp

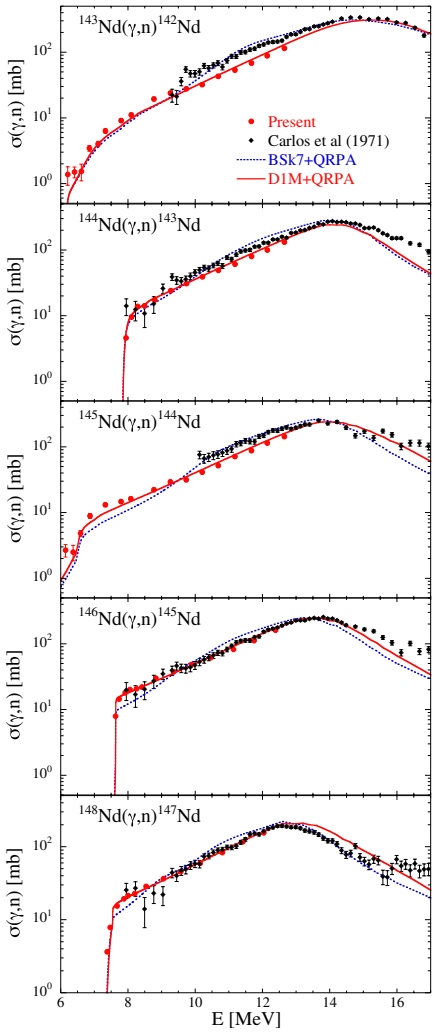

Figure 1. Photoneutron cross sections for Nd isotopes.

3. The γ-ray strength function

3.1. A unified understanding of (γ, n) and (n, γ) reactions

Photoneutron cross sections measured over the Nd and Sm isotopic chain were compared with theoretical calculations obtained by the TALYS nuclear reaction code with two models of γSF, the Skyrme Hartree- Fock-Bogoliubov (HFB) plus quasi-particle random phase approximation (QRPA) model [10] based on the BSk7 interaction and the axially symmetric deformed Gogny HFB plus QRPA model based on the D1M interaction [11]. The experimental data are best reproduced by the latter model of γSF. Figures 1 and 2 show (γ,n) cross sections for Nd and Sm isotopes, reapectively. Figures 3 and 4 show comparisons between the existing (n,γ) cross section data for Nd and Sm isotopes and the TALYS calculations with the D1M+QRPA model of the E1 strength. The shaded area represents the sensitivity to the nuclear level density. Figure 5 shows (n,γ) cross sections for ^{147}Nd with the half-life 10.98 d and ^{153}Sm with the half-life 1.93 d predicted with the same model of the E1 γSF constrained by the (γ,n) cross sections.

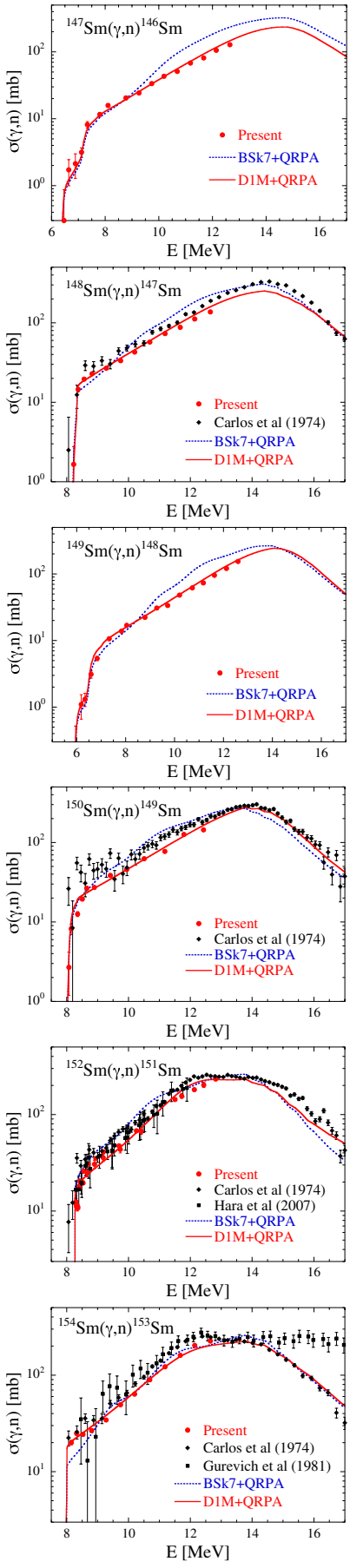

Figure 2. Photoneutron cross sections for Sm isotopes.

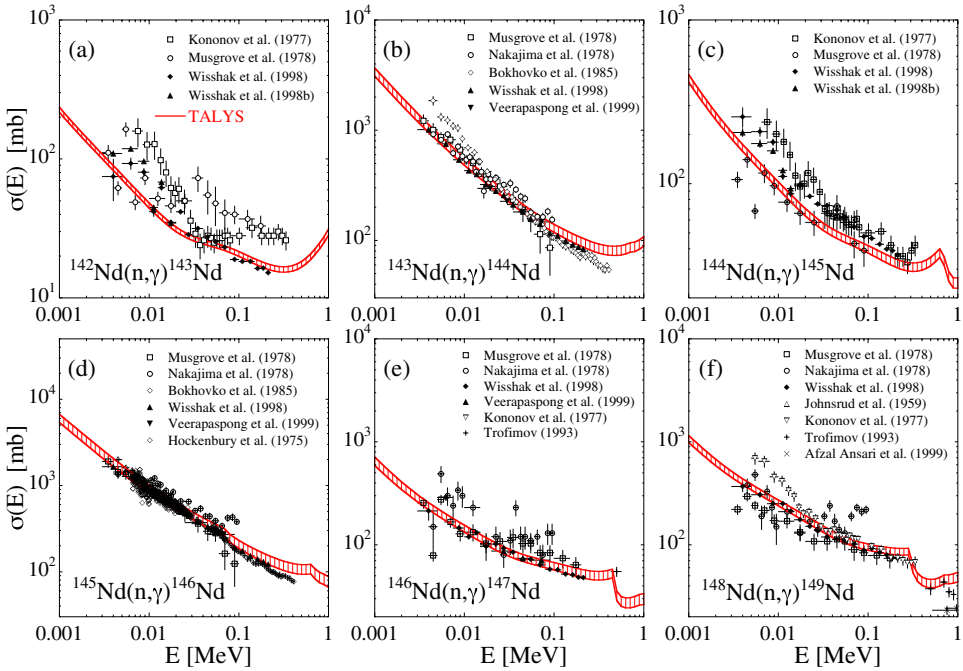

Figure 3. Comparisons of the TALYS calculations with the experimental (n, γ) cross sections for Nd isotopes. The D1M+QRPA model of the E1 strength constrained by the (γ, n) cross sections was used.

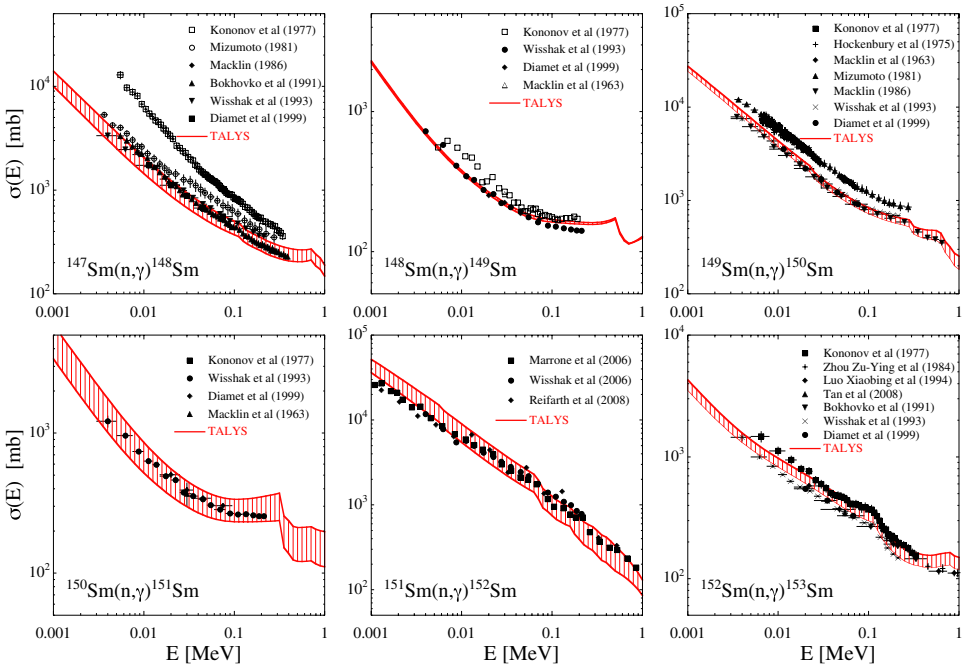

Figure 4. Comparisons of the TALYS calculations with the experimental (n, γ) cross sections for Sm isotopes. The D1M+QRPA model of the E1 strength constrained by the (γ,n) cross sections was used.

3.2. Constructing experimental γ-ray strength function

Experimentally photoneutron cross section measurements provide the upward γSF above the neutron threshold. The nuclear resonance fluorescence measurement provides the downward γSF through the ground-state decay of the populated both resolved and unresolved (quasicontinuum) states below the neutron threshold The Oslo method [12] of deducing the primary γ-transitions from multiple gamma-decay data obtained in inelastic scattering and transfer/pickup reactions can also provide the downward γSF below the neutron threshold. Based on the Brink hypothesis of the approximate equality of the upward and downward γSF, one can construct the γSF by combining (γ,n), (γ,γ') and the Oslo data with the (γ,n) cross section as absolute normalization. Figures 6 and 7 show thus constructed γSF for ^{117}Sn [13] and ^{74}Ge [15].

4. Direct neutron-multiplicity sorting

After the elaborate efforts of evaluating the Livermore and Saclay data of partial photonuetron cross sections, especially those based on the transitional neutron- multiplicity

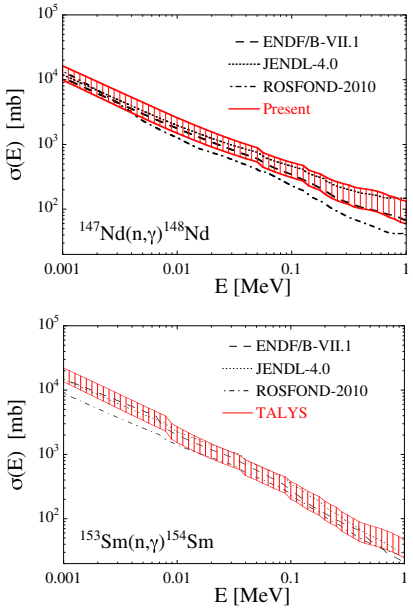

Figure 5. (n, γ) cross sections for ^{147}Nd with the half-life 10.98 d and ^{153}Sm with the half-life 1.93 d predicted with the γ-ray strength function method.

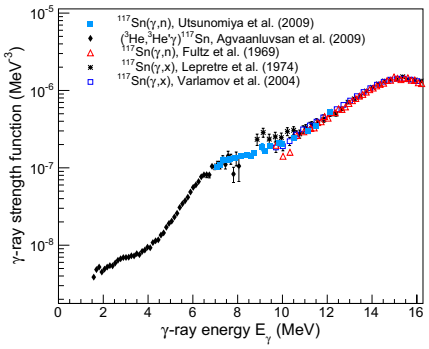

Figure 6. Experimental γ-ray strength function for ^{117}Sn.

function [15] as well as (γ, n) cross sections below two-neutron separation energies compiled in the photonuclear data library [8], it turned out that the discrepancy between the Livermore and Saclay data cannot be resolved in any systematic way. In many cases of the partial cross sections, Saclay provided larger cross sections for (γ, n) reactions than Livermore and vice versa for (γ, 2n) reactions. An important mission of the IAEA-CRP F41032 is to provide new data of total and partial photoneutron cross sections that help resolve the long-standing discrepancy. We propose here direct neutron-multiplicity sorting with a flat-efficiency neutron detector.

4.1. Multi-neutron coincidences vs partial photoneutron reactions

For simplicity, we treat the neutron-multiplicity up to 3. However, the discussion given below holds for any neutron-multiplicity. The number of neutrons, N_x, emitted in the (γ, xn) reaction with the neutron- multiplicity x is expressed by

$$N_x = N_\gamma \cdot N_T \cdot \sigma(\gamma, xn), \quad (1)$$

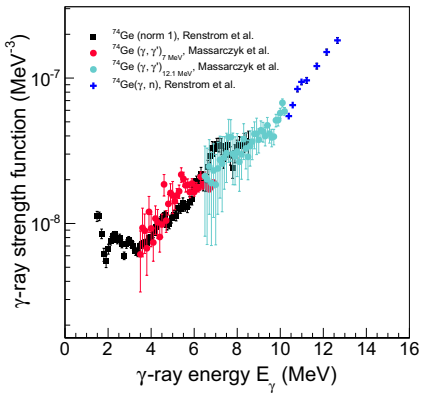

Figure 7. Experimental γ-ray strength function for ^{74}Ge.

where N_γ is the number of γ-rays incident on a target, N_T is the number of target nuclei per unit area, and $\sigma(\gamma, xn)$ is the partial photoneutron cross section. Let us consider a multi-neutron coincidence measurement for (γ, xn) cross sections using a neutron detector with an efficiency ε. We experimentally separate single, double, and triple neutron-coincidence events that are expressed with N_1, N_2, and N_3, respectively, as follows.

$$N_s = N_1 \cdot \varepsilon + N_2 \cdot_2 C_1 \cdot \varepsilon \cdot (1-\varepsilon) + N_3 \cdot_3 C_1 \varepsilon \cdot (1-\varepsilon)^2, \quad (2)$$

$$N_d = N_2 \cdot \varepsilon^2 + N_3 \cdot_3 C_2 \varepsilon^2 \cdot (1-\varepsilon), \quad (3)$$

$$N_t = N_3 \cdot \varepsilon^3. \quad (4)$$

One can see that there are contributions from all (γ, xn) reactions with $x = 1$, 2, and 3 to the single neutron events. The second term, for example, comes from the fact that we can detect one neutron out of two neutrons emitted in the $(\gamma, 2n)$ reaction and undetect the other neutron.

Here we assume that the neutron detection efficiency ε is independent of neutron kinetic energies. When the single-, double-, and triple-neutron coincidence events are experimentally determined, we can solve the set of Eqs. (2), (3), and (4) to obtain N_1, N_2, and N_3 from which $\sigma(\gamma, n)$, $\sigma(\gamma, 2n)$, and $\sigma(\gamma, 3n)$ are determined from Eq. (1).

If the detection efficiency depend on neutron kinetic energies, however, the set of equations become insolvable because neutrons emitted in the $\sigma(\gamma, n)$, $\sigma(\gamma, 2n)$, and $\sigma(\gamma, 3n)$ reactions may have different kinetic energies. For example, the second term on the right-hand side of Eq. (2) is rewritten as $N_2 \cdot \varepsilon(E_{21}) \cdot (1 - \varepsilon(E_{22})) + N_2 \cdot \varepsilon(E_{22}) \cdot (1 - \varepsilon(E_{21}))$ with kinetic energies of the first-emitting neutron (E_{21}) and the second- emitting neutron (E_{21}) in the $\sigma(\gamma, 2n)$ reaction. Note that E_{21} and E_{22} are correlated to each other: the higher the E_{21}, the lower the E_{22}.

The Livermore detector had 45–30% efficiencies over neutron energies up to 5 MeV. The neutron energy dependence of the detection efficiency was still large so that the ring-ratio (RR) technique [16] was used to determine the average neutron energy. The RR technique, which can be applied to multi-neutron coincidence events (N_s, N_d, and N_t), however, does not determine the average neutron energies for individual (σ, xn) reactions.

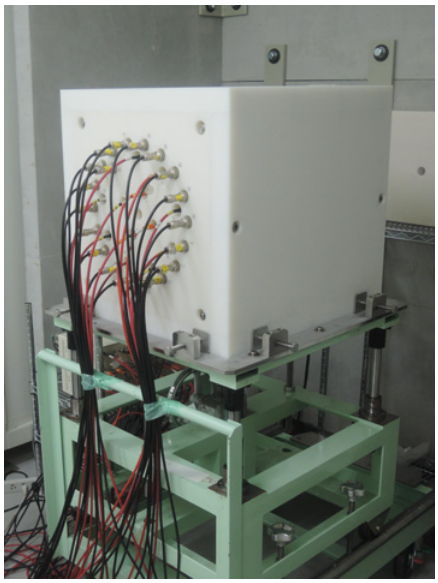

Figure 8. A flat-efficiency neutron detector.

4.2. Flat-efficiency neutron detector

It is essential to develop a flat-efficiency neutron detector to measure partial photoneutron cross sections by direct neutron-multiplicity sorting.

We previously developed a high-efficiency neutron detector (HED) that has efficiencies more than 60% for neutron energies below 1 MeV. This detector has long been used for (γ, n) cross section measurements below two-neutron separation energies. We have newly developed a flat-efficiency neutron detector (FED) by modifying the triple-ring configuration of the HED. The flat response was achieved by weakening the strong-energy dependence of the inner ring, which shows a rapid decrease with increasing neutron energy, at the cost of the large detection efficiency and compensating the energy dependence with increasing efficiencies of the middle and outer rings. The number of ^{3}He counters and the distance of the three rings were optimized by Monte Carlo simulations.

The FED consists of three concentric rings of four, nine, and eighteen ^{3}He counters embedded in a polyethylene moderator at the distances of 5.5, 13.0 and 18.0 cm from the γ-ray beam axis, respectively. The HED and FED share the same ^{3}He counters of 45 cm long active volume filled with a 10 atm gas mixture of ^{3}He and CO_2. Figure 8 shows a picture of the FED.

The efficiency of the FED was calibrated with a ^{252}Cf source whose absolute emission rate was determined to be $(1.62 \pm 0.04) \times 10^4$ neutrons per second at the National Metrology Institute of Japan. The results of the calibration are shown in Fig. 9 in comparison with Monte Carlo simulations. The experimental results are well reproduced by the MCNP [17] simulation (dark lines). The GEANT4 [18] simulations slightly overestimates the efficiency of the inner ring and thus the total efficiency. The total efficiency summed over the three rings is $37.27 \pm 0.82\%$ at 2.13 MeV, the average energy of the ^{252}Cf neutron spectrum and 38.0–32.9% over 0–5 MeV.

Besides the flatness, a reasonably-high efficiency is required in multi-neutron coincidence measurements because the efficiency of detecting i neutrons in coincidences is given by ε^i. The present efficiency assures safely 3- and possibly 4-fold coincidences.

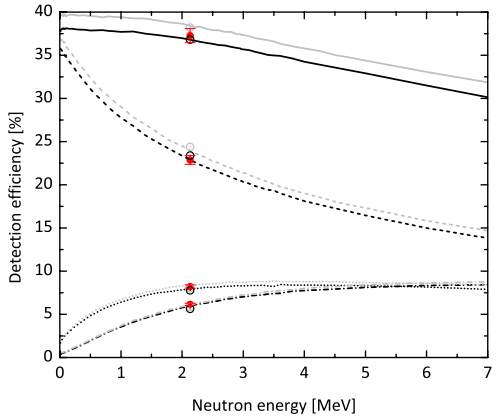

Figure 9. The detection efficiencies of the flat-efficiency neutron detector. Results of the Monte Carlo simulations done with the MCNP (dark lines) and the GRANT4 (grey lines) codes: From the top, the total efficiency, the efficiencies of the inner ring, middle ring, and outer ring.

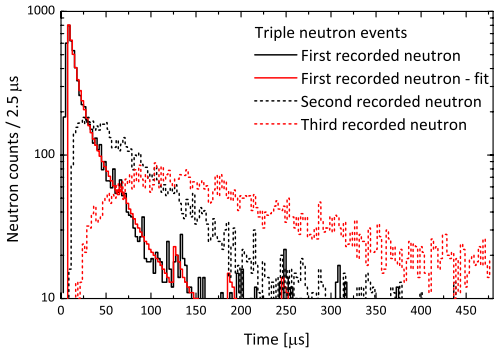

Figure 10. Time-arrival distributions of triple-coincidence neutrons for ^{209}Bi at $E_\gamma = 33.3$ MeV.

4.3. First measurements by direct neutron multiplicity sorting

First measurements by direct neutron-multiplicity sorting were carried out for ^{209}Bi [19] and ^{9}Be at the NewSUBARU facility in 2015.

Figure 10 shows arrival-time distributions of triple-coincidence neutrons detected with the ^{3}He counters after moderation in the polyethylene for ^{209}Bi at $E_\gamma = 33.3$ MeV. A detailed analysis of the multiple- neutron events is in progress.

5. The PHOENIX collaboration for the IAEA-CRP

The PHOENIX, which stands for "**pho**to**e**xcitation and **n**eutron em**i**ssion cross (**x**) sections" collaboration for the IAEA-CRP has begun at the NewSUBARU facility in Japan. Four teams of the Konan University, the ELI-NP [20], the University of Oslo, and the Lomonosov Moscow State University are formally involved in this collaboration. We measure (γ, n) cross sections for the IAEA-CRP of generating a reference database for photon strength functions and (γ, xn) cross sections with x = 1–3 for that of updating the photonuclear data library.

The Konan, ELI-NP, MSU, and Oslo teams are officially assigned their own (γ, xn) and (γ, n) data within the IAEA-CRP F41032 as follows.

1. (γ,xn) data with x = 1 – 3 for 11 nuclei for updating the photonuclear data library

The Konan team: ^{197}Au, ^{181}Ta, ^{139}La, ^{9}Be

The ELI-NP team: ^{209}Bi, ^{169}Tm, ^{165}Ho, ^{159}Tb

The MSU team: ^{103}Rh, ^{89}Y, ^{59}Co

2. (γ,n) data for 18 nuclei for generating a reference database for photon strength functions

The Konan team: ^{160}Gd, ^{158}Gd, ^{157}Gd, ^{156}Gd, ^{64}Ni, ^{60}Ni, ^{58}Ni

The Oslo team: ^{205}Tl, ^{203}Tl, ^{192}Os, ^{185}Re, ^{184}W, ^{183}W, ^{182}W, ^{89}Y, ^{68}Zn, ^{66}Zn, ^{64}Zn

In addition to the official assignment, the PHOENIX collaboration may go beyond the IAEA-CRP, depending on the availability of enriched samples. Additional data of (γ,n) cross sections were obtained for four nuclei, ^{138}Ba, ^{137}Ba, ^{61}Ni, and ^{13}C in 2016.

I.G. and D.F. acknowledge the support from the Extreme Light Infrastructure Nuclear Physics (ELI-NP) Phase II, a project co-financed by the Romanian Government and the European Union through the European Regional Development Fund - the Competitiveness Operational Programme (1/07.07.2016, COP, ID 1334). This work was supported by the IAEA under contracts 20476 and 20501 for the CRP on Updating the Photonuclear Data Library and generating a database for Photon Strength Functions.

References

[1] D.M. Brink, Ph.D thesis, Oxford University, 1955
[2] H. Utsunomiya et al., Phys. Rev. C **82**, 064610 (2010)
[3] H. Utsunomiya et al., Phys. Rev. C **81**, 035801 (2010)
[4] H. Utsunomiya et al., Phys. Rev. C **84**, 055805 (2011)
[5] H. Utsunomiya et al., Phys. Rev. C **88**, 015805 (2013)
[6] D. Filipescu et al., Phys. Rev. C **90**, 064616 (2014)
[7] H.-T. Nyhus et al., Phys. Rev. C **91**, 015808 (2015)
[8] *Handbook on photonuclear data for applications. Cross-sections and spectra, Final report of a coordinated research project 1996 – 1999*. IAEA-TECDOC-1178, 2000
[9] S.S. Dietrich and B.L. Berman, At. Data and Nucl. Data Tables **38**, 199 (1988)
[10] S. Goriely, E. Khan, and M. Samyn, Nucl. Phys. A **739**, 331 (2004)
[11] M. Martini, S. Hilaire, S. Goriely, A. J. Koning, and S. Péru, Nucl. Data Sheets **118**, 273 (2014)
[12] A. Schiller et al., Nucl. Instrum. Phys. Res. A **447**, 498 (2000)
[13] U. Agvaanluvsan et al., Phys. Rev. Lett. **102**, 162504 (2009)
[14] T. Renstrøm et al., Phys. Rev. C **93**, 064302 (2016)
[15] V.V. Varlamov, B.S. Ishkhanov, V.N. Orlin et al., Eur. Phys. J. A **50**, 114 (2014)
[16] B.L. Berman and S.C. Fultz, Rev. Mod. Phys. **47**, 713 (1975)
[17] J.F. Briesmeister, computer code MCNP, Version 4C (Los Alamos National Laboratory, Los Alamos, 2000)
[18] J. Allison et al., IEEE Trans. Nucl. Sci. **53**, 270 (2006)
[19] I. Gheorghe et al., S478 in this conference
[20] `www.eli-np.ro`